Three-dimensional reconstruction of a periodic free surface from digital imaging measurements

D. Devriendt[1], D. Douxchamps[2], H. Capart[1,3], C. Craeye[2], B. Macq[2] & Y. Zech[1]

[1] *Dept. of Civil Engineering, Univ. Catholique de Louvain, Bât. Vinci, Pl. du Levant 1, B-1348 Louvain-la-Neuve, Belgium*

[2] *Communications and Remote Sensing Lab., Univ. Catholique de Louvain, Bât. Stévin, Pl. du Levant 2, B-1348 Louvain-la-Neuve, Belgium*

[3] *Fonds National de la Recherche Scientifique, Belgium*

Abstract

We report on imaging techniques aimed at the three-dimensional characterisation of a fast-flowing free surface. The flow considered is a shallow-water current propagating over a gradually varied train of antidunes. Nearly periodic surface waves develop as a result of interaction with the three-dimensional bedforms. The topography of the flow free surface constitutes the primary interest. Two measurement techniques are presented, one direct based on stereovision, and one indirect based on velocimetry and fluid mechanical constraints. Preliminary results obtained using the two techniques are compared. Both methods are shown to yield free-surface geometries at resolutions much higher than those attainable using conventional gauges.

1 Introduction

Surface wave fields that are highly varying in time and space constitute challenging phenomena for experimental fluid mechanics. Point measurements provided by arrays of wave gauges or pressure transducers, in general, yield low resolution data which are sometimes difficult to compare with theoretical or numerical models. In addition,

these techniques often require the positioning of instruments inside or directly in contact with the flow, thereby potentially interfering with the phenomena under study.

For shallow-water currents over wavy sediment beds, and in particular at the torrential regime considered in the present paper, both problems can be quite significant. First, as a result of coupling between the flow and the migrating antidunes formed by the bed, the free surface develops an organised three-dimensional pattern which is hard to capture using sparsely sampled measurements. Secondly, the local morphodynamics of the sand bottom are very sensitive to intruding instruments.

Such phenomena, therefore, constitute applications where whole field, remote sensing methods can be highly valuable [8]. In what follows, we present digital imaging techniques geared towards that aim which are currently under development as part of a research on sand waves and non-equilibrium sediment transport. Specifically, we focus here on the free surface topography problem, i.e. the reconstruction of the three-dimensional geometry of the flow surface. Both direct and indirect measurement techniques are explored, based on the imaging of floating tracers.

In the first technique, the surface geometry is reconstructed directly from stereoscopic views provided by two commercial digital cameras. The main challenges of this method lie in achieving a good calibration and synchronisation of the twin cameras, and in correctly matching particles between views.

In the second technique, an indirect estimation is sought based on velocimetry measurements. Digital particle velocimetry is first used to obtain the horizontal velocity components from images acquired using a single high-speed camera. The free-surface geometry is then reconstructed by solving an inverse problem based on fluid mechanical constraints. This can be achieved with a surprisingly simple formulation, based on a first order perturbation of the Bernoulli equation applied streamline by streamline.

2 Experimental set-up and flow conditions

The experiments were conducted in a sediment flume 6 m long and 50 cm wide, with the latter dimension sufficient to prevent antidunes

Transactions on Engineering Sciences vol 18, © 1998 WIT Press, www.witpress.com, ISSN 1743-3533

from being constrained too tightly by the sidewalls. A coarse sand of nearly uniform size distribution was used as sediment material. The flows observed had their Froude number in the range $Fr = 1.4 - 1.6$, at which antidunes present a strong three-dimensional character [1,7].

Image sequences were obtained using digital cameras placed above the flow as shown by the sketches of figure 1. For the stereometry measurements, two commercial digital cameras were used to capture the flow at a rate of 25 images per second. The velocimetry measurements, on the other hand, were extracted from image sequences acquired at a frame rate of 250 images per second using a high-speed, single camera system. For both methods, the flow free surface was seeded with floating tracers consisting of black and white wooden pearls 9 mm in diameter.

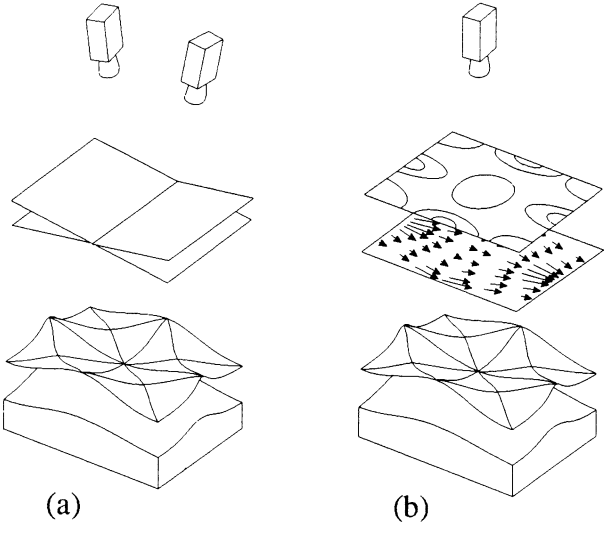

Figure 1: Measurement principles and camera configurations: (a) Stereometry; (b) Geometry from velocimetry.

The success of the image analysis process depends on a large measure on a careful control of the illumination. As of yet, we have not found lighting conditions suitable for a simultaneous use of both camera systems, which means that the preliminary results presented below for the two techniques were obtained for distinct flows and can only be compared in a qualitative way.

3 Particle localisation

For both reconstruction techniques, the first step of the analysis is the identification of the particles on the digital frames, isolating them from the surrounding fluid. Because the illumination obtained was not perfectly uniform over the viewing window, and because of the irregularities due to the underlying sediment bed and specular reflections on the water surface, a simple threshold in light intensity was not enough to discriminate the particles from their neighbourhood. Instead, a method inspired from [4] and [9] was used. It relies on convoluting the grey level images with a Laplacian of Gaussian mask (see [6]), which highlights the zones of radial symmetry corresponding to tracer particles. Subpixel accuracy was achieved by interpolation around local maxima of the convoluted images.

4 Stereometry

4.1 Calibration and synchronisation of the cameras

The key preliminary step of stereoscopic analysis is camera calibration, by which the projection parameters relating image coordinates to world coordinates are defined for the two cameras. In the present application, this was done independently for each one, under the assumption that the projection can be modeled as an affine transformation within the image plane [6]. A cube of known dimensions, placed in the viewing volume of both cameras before the experiments, served as referential for a first calibration. A set of 50 recognisable points in both views was then chosen to calibrate the transformation a second time and improve the robustness of the subsequent matching.

Accurate synchronisation of the two cameras is also essential for topographic measurements of fast flows such as those considered here. This is because the distance covered by particles between non-synchronised views will result in an artificial stereoscopic effect contaminating the elevation measurements (the same effect as the one exploited by Cameron [3] to measure current velocities from aerial photographs). In the absence of a synchronising board, a reasonable correspondence (to within 1/100 s) was obtained by placing a counter display in both cameras' shared viewing volume.

4.2 Matching and positioning of stereo pairs

Stereoscopic reconstruction requires matching conjugate pairs of particles between the two views. As the free surface, in first approximation, undulates around a mean plane parallel to the mean bed slope, it is possible to perform the matching by simply projecting the particle images of both cameras on this imaginary plane, then matching the projections closest to one another. Discrepancies between the two projections of a conjugate pair then indicate elevation above or below the chosen mean plane. The three-dimensional position of each particle is finally obtained as the median of the segment of minimum distance between the rays associated with the two conjugate particle images. Conspicuous outliers (resulting from mismatches) are eliminated before proceeding to surface regularisation.

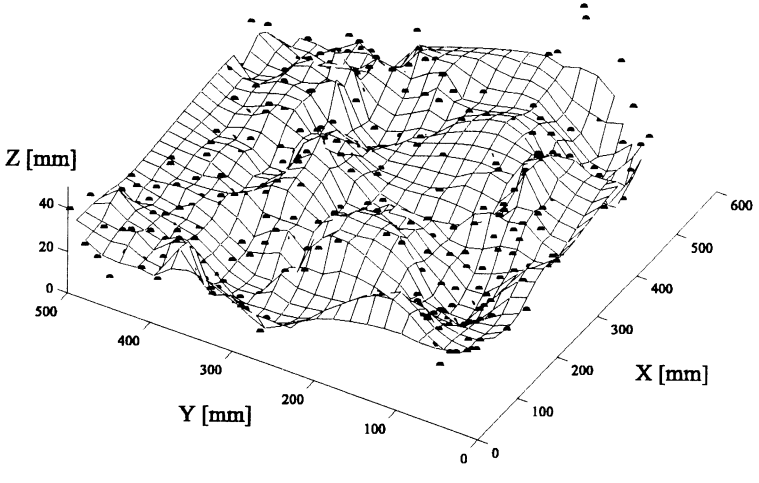

Figure 2: Stereoscopic points and interpolated surface

4.3 Regularisation procedure

The matching of stereo pairs described above produces a set of points in space which approximately belong to the desired flow free surface (figure 2). Because of inaccuracies (in localisation, calibration, synchronisation,...), however, the points inevitably present some degree of scatter. A final operation therefore consists in the application of

a regularising procedure. Aside from small scale surface roughness, the physical water surface is expected to be reasonably smooth, so that a regularised three-dimensional surface can be constructed on an evenly spaced grid by minimising the functional [6]:

$$F\Big(Z(X,Y)\Big) = \sum_k \Big(Z(X_k,Y_k) - Z_k\Big)^2 + \beta^2 \iint_{\mathcal{D}} \Big(\nabla^2 Z\Big)^2 \, dX\,dY \quad (1)$$

where Z is the regularised surface elevation perpendicular to the mean bed plane, (X,Y) are the coordinates in that plane, (X_k,Y_k,Z_k) are the points obtained from the matching procedure, and β is a weight coefficient regulating the amount of smoothing desired. This variational problem can be cast into its Euler-Poisson differential formulation, which is then easily solved by finite differences [5,6].

5 Geometry from velocimetry

5.1 Reconstruction principle

The indirect method proposed here relies on a simple measurement principle which to our knowledge has not yet been exploited for this type of application. The reasoning will be sketched here in a heuristic manner, but can be derived more rigorously.

Since the bed morphology evolves slowly with respect to the flow velocity, we can reasonably consider that the flow behaves in a quasi-steady fashion. Along a surface streamline (identical to the pathlines of particles since the flow is considered quasi-steady), neglecting dissipation and mean slope terms, we can express the Bernoulli equation as

$$\frac{\vec{V}\cdot\vec{V}}{2g} + Z = \text{constant along a streamline} \quad (2)$$

where $\vec{V} = (U,V,W)$ is the velocity. We can then consider that the flow over antidunes can be described, in first approximation, as small fluctuations around a mean uniform flow in the X direction and write

$$\frac{\widetilde{U}(U-\widetilde{U})}{g} + (Z - \overline{Z}) \approx 0 \quad (3)$$

where the tilde denotes an average over a streamline and the overbar an average over the entire flow region. In deriving (3), we have considered that the velocity fluctuations following the three directions are

all of the same order and much smaller than $\widetilde{U}$. Also, it is because a uniform flow along the X direction presents a horizontal surface in the transverse direction Y that we have been allowed to consider $\widetilde{Z} = \overline{Z}$. If the horizontal velocities are known along streamlines, expression (3) offers a way of estimating elevation with respect to the mean surface plane. Basically, the behaviour of streamline particles, moving slower over the crests and faster in the troughs, is analogous to the motion of spheres rolling on a solid wavy surface.

5.2 Particle tracking and streamline processing

Providing a way of obtaining particle pathlines from sequences of digital images, particle tracking techniques [1] constitute ideally suited tools for the present purpose. By placing a single camera above the flow, with its image plane parallel to the mean free surface, and automatically tracking particles from one frame to the next, we can directly estimate the projected trajectories and horizontal velocity components.

Figure 3 shows forty streamlines obtained in this way from image sequences. They form a pattern which is typical of flows over antidunes, with streamlines converging at the flow crests where the flow is deeper [2].

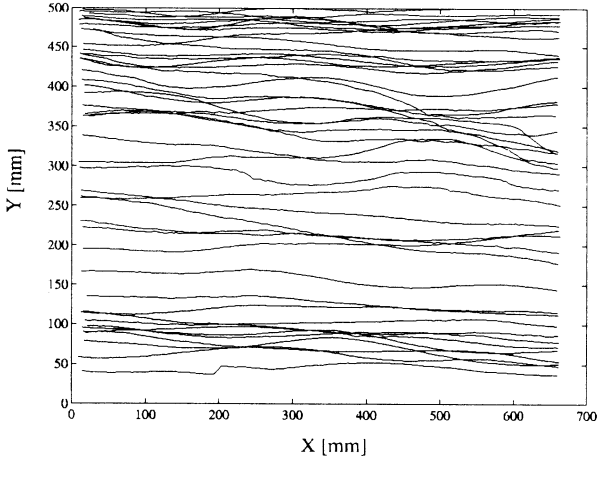

Figure 3: Streamlines obtained by particle tracking

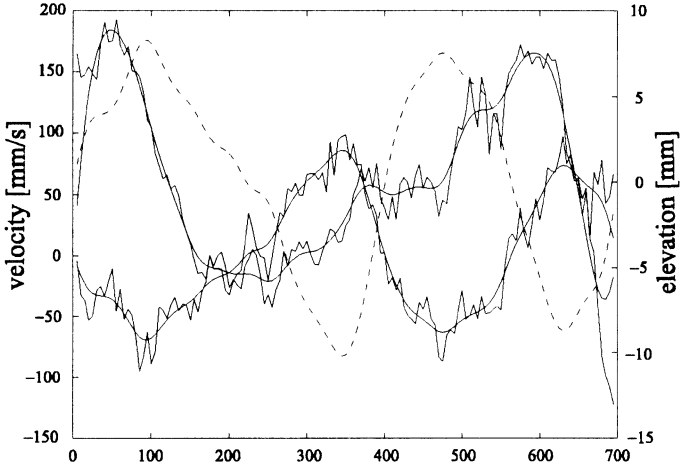

Figure 4: Measured velocities (—) and derived elevation (- -) along a streamline

Figure 4 presents the measured time evolution of the (U, V) velocity components, as well as the corresponding elevation $(Z - \overline{Z})$ obtained from equation (3). Velocities are shown as raw data and as regularised curves obtained by minimising the one-dimensional equivalent of functional (1).

6 Results and discussion

Complete surface plot results of the regularised surfaces obtained by stereometry and by velocimetry are shown on figure 5. The experimental conditions were not identical for the two cases, so that it is not the particular wave configurations but the overall patterns and resolutions of the two surfaces which should be compared. Features of the measured surfaces such as the positions of the peaks and the amplitudes of the undulations match those that were visually observed during the experiments.

The surface patterns shown are characteristic of three-dimensional antidunes [2], with the free surface locally peaked up into short-crested waves. The wavelengths given by the measurements also agree well with a theoretical relation for three-dimensional antidunes given by Kennedy (quoted in [2]):

$$\overline{U}^2 = \frac{g\lambda_a}{2\pi}\left(1 + (\lambda_a/S)^2\right)^{1/2} \tag{4}$$

in which λ_a is the wavelength (along X) and S is the span of the surface waves.

Given their high resolution, it is also seen that much more information could actually be extracted from the obtained measurements. Finally, it should be possible to use these methods to characterise the time evolution of non-equilibrium bedform fields.

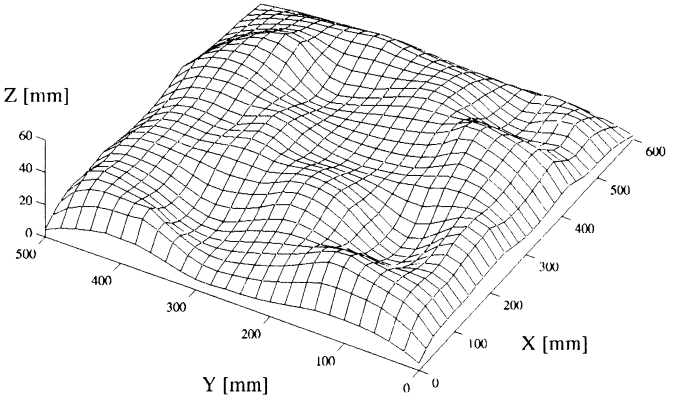

(a)

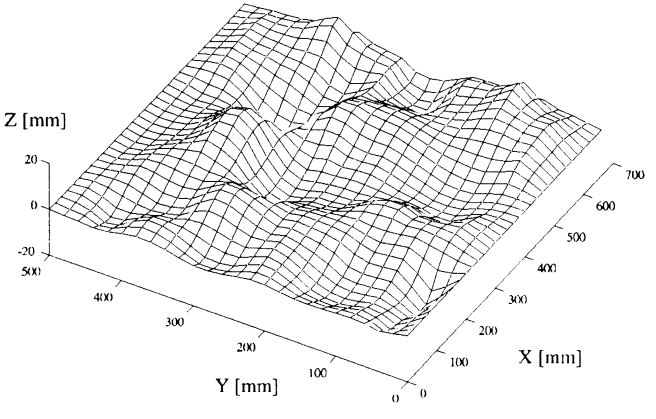

(b)

Figure 5: Regularised free surfaces derived (a) from stereometry data;(b) from velocimetry data. (Note: the two sets of data correspond to distinct experimental runs.)

The authors are grateful to Olivier Cantineau, of the Microelectronics Laboratory, and Bernard François, Unité de Thermodynamique et Turbomachines, UCL, for their help with the camera systems.

References

[1] Adrian, R.J., Particle-Imaging Techniques for Experimental Fluid Mechanics, *Annual Review of Fluid Mechanics*, **23**, pp. 261-304, 1991.

[2] Allen, J.R., *Current Ripples: Their Relation to Patterns of Water and Sediment Motion,* North-Holland, Amsterdam, pp. 34-36, 1968.

[3] Cameron, H.L., The measurement of water current velocities by parallax methods, *Photogrammetric Engineering*, **18**, pp. 99-104, 1952.

[4] Capart, H., Liu, H.H., Van Crombrugghe, X. & Young, D.L., Digital Imaging Characterization of Water-Sediment Interaction, *Water, Air and Soil Pollution*, **99**, pp. 173-177, 1997.

[5] Elsgolc, L.E., *Calculus of Variations,* Pergamon, London, 1962.

[6] Jain, R., Kasturi, R. & Schunck, B.G., *Machine Vision,* McGraw-Hill, New York, 1995.

[7] Kennedy, J.F., The mechanics of dunes and antidunes in erodible-bed channels, *Journal of Fluid Mechanics*, **16**, pp. 521-544, 1963.

[8] Peakall, J., Ashworth, P. & Best, J., Physical Modelling in Fluvial Geomorphology: Principles, Applications and Unresolved Issues, Chapter 9, *The Scientific Nature of Geomorphology,* eds. B.L. Rhoads & C.E. Thorn, Wiley, Chichester, pp. 221-253, 1996.

[9] Strickland, R.N. & Hahn, H.I., Wavelet Transform Methods for Object Detection and Recovery, *IEEE Transactions on Image Processing*, **6**, pp. 724-735, 1997.